*Journal of Hazardous Materials*, 7 (1983) 87—112
Elsevier Scientific Publishing Company, Amsterdam — Printed in The Netherlands


# ON THE STRUCTURE OF INSTANTANEOUS PLUMES IN THE ATMOSPHERE

C.D. JONES
*CDE Porton Down, Salisbury, SP4 0JQ (Gt. Britain)*
(Received March 30, 1982; accepted May 21, 1982)

## Summary

Current methods for the analysis and prediction of the concentration fluctuations occurring in substances dispersing in the atmosphere are reviewed particularly with reference to existing experimental data.

The results obtained from a series of very high time resolution concentration measurements conducted in neutral conditions over flat terrain using specially developed tracer techniques are then examined in detail. Various statistical, and other parameters, are formulated and quantified in an attempt to characterize the observations. The implications for dispersion modelling, particularly in situations where fluctuations are important i.e. in the evaluation of risks due to flammable, toxic or reactant materials and of nuisance due to malodourous substances are then considered.

It is evident that risk/hazard analyses based on time mean concentrations distributions can at best be misleading and at worst result in serious underestimation when fluctuation-sensitive phenomena are involved.

## 1. Introduction

The use of Gaussian (or similar mathematical form) descriptions for the crosswind and vertical concentration/dosage profiles in atmospheric dispersion models is a well established and widespread practice and the fact that such profiles arise in an apparently natural way as solutions to the 'equations of turbulent diffusion' confers upon them a degree of respectability which is undeserved. The reason for this is that these equations are not precise mathematical representations of physical phenomena: they are based on an analogy not of mechanism but rather of result between molecular and turbulent dispersion processes. Nevertheless in some situations, generally those in which the longer term aspects of exposure to pollutants are of concern and the effect of concentration upon 'response' is linear, predictions based on these techniques yield results which accord reasonably well with experiment and are thus helpful. However the uncritical acceptance of the molecular: turbulent dispersion analogy can, if applied inappropriately, give rise to very misleading estimates of the concentration fields expected in the vicinity of pollutant sources. Closer scrutiny reveals that the disparity between prediction

and reality can be traced to the fact that the implied physical similarity between molecular and turbulent dispersion processes can only be a sensible hypothesis when the spatial scale of relevance to the problem (i.e. the size of the dispersing cloud and/or that of the detector) is considerably greater than the elements (i.e. eddies) actually causing the dispersion. If this is not so then those eddies which have scales of similar size to the cloud itself or are larger will cause it to move bodily thereby resulting in large, rapid and unpredictable (at least on a conventional Gaussian model) fluctuations in concentration.

Hence, if it is the 'instantaneous' concentration experienced at a particular point which is important, as for example it would be in examining a flammability, toxic or malodour problem, then it is vital to bear in mind the limitations of most of the currently used methods of analysis. Whilst some allowance can be made by introducing semi-empirical adjustments to the model predictions to account for the physical fact that instantaneous concentrations can, and do, exceed Gaussian mean values by substantial factors such a procedure is not satisfactory. This is because an approach of this type avoids any attempt to quantify the *mechanism* of the processes responsible for causing the fluctuations. The main theoretical difficulty arises from the fact that material released from a source is initially advected away in the direction of the instantaneous wind vector and this latter varies continuously in magnitude and direction. (This very obvious feature of atmospheric dispersion is immediately confirmed by a few minutes' observation of an industrial stack or similar plume.) Also evident, and of considerable importance because it implies the existence of high local concentrations, is that the plume *itself* is frequently not very well dispersed but consists of a long sinuous volume of material.

Consequently, if the concentration of plume material is measured with a sufficiently rapid response detector a series of relatively short bursts of high concentration are seen interspersed with generally rather longer intervals during which the concentration is either zero or very close to zero. Figure 1 illustrates this point. Csanady [1] refers to this phenomenon as intermittency (note that Townsend [2] introduced this concept, in relation to a turbulent velocity field, much earlier) and suggests that it may be quite normal for the concentration to be zero at a given sampling point for up to 80% of the observation time: a feature subsequently confirmed by the writer (Jones [3]) in some recent experiments. Alternatively, if the *time averaged* concentrations are observed, using for example dosage type receptors at a set of locations distributed in a horizontal arc about the mean wind vector (i.e. mean plume axis) then, provided the sampling time exceeds the longest significant eddy scale ($\sim$ 15 mins) an *approximately* Gaussian spatial profile of dosage will probably result. It was of course this discovery which reinforced the development and exploitation of the analogy between molecular and turbulent phenomena discussed above.

Recognition, particularly recently, of the inherent deficiencies in current

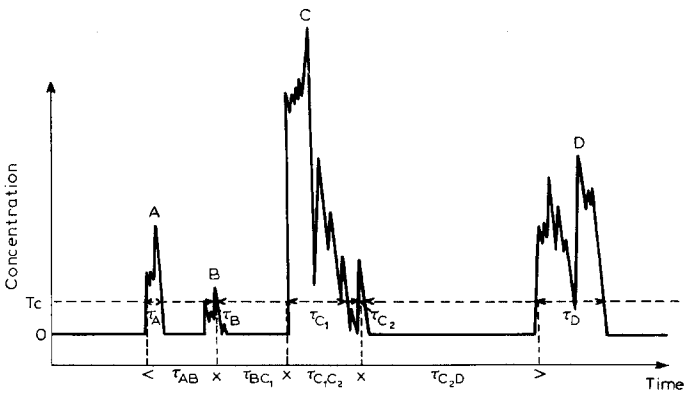


Fig. 1. Illustrating the use of CAAS (Concentration Amplitude Analysis System) and SHADA (Signal Height and Duration Analyser).

dispersion modelling procedures has stimulated a reexamination of the experimental data available in order to develop physically more realistic approaches to the analysis of fluctuation sensitive phenomena. However, lack of high resolution sampling techniques has hindered the exploration of this aspect of atmospheric dispersion and very little data exist on which to base more refined models. Certainly many qualitative observations (and remarks) have been made concerning the fluctuating properties of plumes, but apart from a few isolated exceptions (see next section) there has been no attempt to develop theories capable of explaining or predicting fluctuation structure.

In the last two or three years however several atmospheric dispersion programmes have been carried out by the writer and others [e.g. 3, 4] using a novel tracer method capable of better than $10^{-2}$ s resolution. These two earlier papers have outlined some of the more basic aspects of instantaneous plume structure and have produced direct evidence for the existence of heterogeneities in concentration down to very small scales — a few centimetres — thereby implying very large spatial gradients of concentration. This paper re-examines the nature of these and other features in a more penetrating manner and in particular attempts to derive reliable quantitative data from the experimental results which are more directly applicable to modelling. It should be emphasised however, that the intention cannot be to promulgate definitive information on the fluctuations and the parameters describing them because this would require a much larger experimental data base than is currently available before precise statements could be made. Rather it is to provide reasonably reliable indications of the type of distributions that are likely to be encountered in practice.

## 2. Earlier experimental investigations and their impact on theories of cloud structure

The theoretical formulation of rigorous descriptions of atmospheric

plume and puff structure can only be contemplated in statistical terms. It is possible that, eventually, realistic estimates of peak concentration and related 'instantaneous' parameters will be feasible at least in reasonably straight forward situations. It will, however, remain difficult to ascribe confidence levels to such estimates and it is to be expected that a substantial proportion of the theory will develop in an ad hoc and empirical fashion to explain what is observed. Many of the problems in formulating statistical models of plume or puff structure are related to two characteristic features of atmospheric turbulence: namely its spatial inhomogeneity (e.g. arising from surface irregularities) and its temporal non-stationarity (due mainly to synoptic and diurnal influences). These properties, whilst implicit of course and effective in the earliest dispersion experiments, were not so relevant then because of the preoccupation with dosages and long term average concentration distributions.

A consequence of the above is that the fundamental concept underlying the analysis and characterisation of instantaneous concentration properties has therefore, of necessity, to be that of the ensemble, rather than a spatial or temporal, average. Clearly one cannot in practice perform ensemble type experiments*, i.e. to release material and observe the ensuing concentration at a series of points in space-time (the latter in the relative sense) repeatedly. Reasonable, and indeed the only practical, alternatives one can conceive are experiments in which, with spatially homogeneous conditions, many sources and detectors are deployed sufficiently well spaced for the results to be statistically independent and the concentrations noted at a given time; or, in temporally stationary conditions, the statistics could be built up by observing the concentration at a single detector as a function of time. Obviously the latter is the preferred option since it is far less demanding on experimental resources; however, there remains the inherent difficulty of developing an acceptable criterion for defining stationary or at least quasi-stationary conditions. In practical terms this necessitates avoiding, in clear weather, the hours near sunrise and sunset when the stability undergoes marked and rapid changes. Also conducting experiments in which mesoscale (e.g. showers, thunderstorms) and synoptic (e.g. fronts) events are taking place is precluded.

Chatwin [5], in his 1982 paper, discusses a mathematical analysis which although intended for puffs, can be satisfactorily extended to plumes by suitable redefinition of the parameters concerned. Retaining his notation, consider the concentration at a point $x$ in coordinates relative to the source at a time $t$. Suppose the value of concentration observed in the $r^{\text{th}}$ experiment is $\Gamma^{(r)}(x, t)$ then, by definition, the ensemble mean,

$$C(x, t) = \lim_{n \to \infty} \frac{1}{n} \sum_{r=1}^{n} \Gamma^{(r)}(x, t) = \overline{\Gamma}(x, t) \tag{1}$$

*i.e. in the field, however one could conceive and enact experiments of ensemble type in the laboratory and then attempt to apply the results to atmospheric situations by invoking appropriate scaling laws.

In *completely* stationary conditions the ergodic hypothesis may be invoked and the ensemble mean can be expressed in the form of a time integral,

$$C(x) = \frac{1}{T} \int_0^\infty \Gamma\,(x,\, t)\, \mathrm{d}t, \tag{2}$$

which is independent of $t$.

Equations 1 and 2 are not informative regarding the fluctuations per se and to specify their characteristics it is necessary to investigate the behavious of the higher moments of $\Gamma\ (x,\ t)$, and strictly this should be done in the ensemble context.

Prior to proceeding it is helpful to consider in more detail how the mean concentration is actually accumulated over a period of time. Observations with high-resolution tracer techniques by Barynin and Wilson [6], Hadjitofi and Wilson [7] and Jones [8] downwind of various types of atmospheric sources have unequivocally shown the intermittent nature of $\Gamma\ (x,\ t)$. In the simplest situation of a single detector it was found that for a significant fraction, normally the majority, of the observation period the concentration was zero — i.e. the detector was not in the plume at all. (Recognition of this fact earlier led Gifford [9] to propose his fluctuating plume model which was, however, based on 'Gaussian' concpets.) In addition, the experiments indicated the presence of considerable amounts of fine structure actually within the plumes themselves and, even at 5 km downwind from the source, heterogeneities of remarkably small-scale were found.

Taken together these experimental findings convey a substantially different impression of a plume than would be deduced from Gaussian models. In particular, due to the discontinuous nature of the concentration field, the use of conventional descriptors of fluctuation characteristics (i.e. the higher statistical moments) is somewhat questionable. Never theless, providing such techniques are applied and interpreted intelligently, they are capable of specifying certain features of the fluctuations in a reliable and therefore helpful manner. In stationary conditions the $n^{\text{th}}$ central moment, denoted by $M_n(x)$ is defined as

$$M_n(x) = \frac{1}{T} \int_0^\infty [C(x) - \Gamma\ (x,\ t)]^n\ \mathrm{d}t \tag{3}$$

It is often convenient to express the second moment (i.e. the fluctuation variance) in non-dimensional form so that direct comparisons between experiments are facilitated. One thus defines the relative intensity of the fluctuations, $I(x)$, as

$$I(x) = \sqrt{M_2(x)}/C(x) \tag{4}$$

Normalized third and fourth moments, the skewness and kurtosis respectively, also provide valuable information on the character of the fluctuations — i.e. their shape and "peakiness". Note, however, that certain problems can arise in the determination of these moments, particularly the latter, because lengthy observation periods are required in order to establish stable values (see Lumley and Panofsky [10]) and these are generally precluded by the need to collect data in as near stationary conditions as possible.

One aspect of the observed concentration data that necessitates particular consideration is the approach to handling the intervals, which are often lengthy, when the concentration is zero or at least less than some very small value. It is evident that for the calculation of the second and higher moments inclusion of very many zeroes would tend to confuse the results by introducing large contributions into the integrals which had nothing whatever to do with the nature of the *fluctuations themselves.* Hence a pragmatic approach was taken, which though somewhat hard to defend rigorously, did enable realistic values of these moments to be obtained. This was achieved by adopting a conditional sampling procedure in which integration was only carried out when $\Gamma(x, t) > 0$*.

Concentration-frequency distributions provide additional information on plume structure and, in many cases, logarithmic-normal cumulative probability distributions have been fitted to sequences of observed data [e.g. 1, 11]. Although the theoretical justifications for compliance with this particular distribution are fairly vague there is, as yet, no other distribution which appears to offer a better fit to the available data. An argument against the use of the log-normal distribution is that all the zero values of concentration have to be discounted before the fluctuation data can be fitted — hence this distribution really describes a distribution *within* the plume and not that experienced at a particular sampling point.

The experiments of Barynin and Wilson [6], using methyl mercaptan ($CH_3SH$) as the 'tracer' and fast-response detectors revealed various interesting features about odour perception which relate directly to plume structure. Rapid rises in concentration were found to be especially noticeable when compared with similar variations occurring over a longer time interval. This is significant because the leading, i.e. oncoming, edges of plumes (and puffs) frequently exhibit very rapid increases in concentration (probably reinforced by the shear processes occurring) and hence olfactory response appears well adapted to providing the maximum warning of the arrival of unpleasant (or, more importantly, dangerous) airborne material. It was also found, and this is known from everyday experience, that response declines on prolonged exposure to odour but is restored if the stimulus is temporarily withdrawn and then re-presented. Thus, to summarize, the nose is well attuned to respond efficiently to the two most significant features of instantaneous concen-

*Note: Single point measurements are the only type discussed in this paper; multi-point statistics will form the subject of a later publication.

tration fields: i.e. the presence of large spatial gradients and the existence of considerable intermittency.

The rate of presentation of stimuli is important not only from the odour nuisance assessment standpoint but also in the study of a variety of biological processes, e.g. the insect pheromone sex-attractant mechanism, as discussed by Murlis and Jones [4]. In these processes it may be possible to consider the response in a quantized, possibly even binary, fashion — i.e. nothing happens below a given threshold concentration whilst some particular activity occurs once that threshold is exceeded. (Certainly in the human case the threshold of odour perception varies considerably among individuals and, thus in establishing the likely level of odour nuisance, a more sophisticated analysis will be required.)

The implication of these findings is therefore that a rather different type of data analysis is required than provided by the approaches outlined earlier. Information on the temporal, as opposed to the amplitude, structure of the fluctuations in the form of peak duration and, just as important, gap-length distribution might therefore provide a basis on which to develop more realistic descriptions of plume structure appropriate for odour nuisance assessment etc. In effect the analysis involves investigating the relation

$$\sum_{i=1}^{n_{pi}} t_{pi} + \sum_{j=1}^{n_{gj}} t_{gj} \; (=T) \tag{5}$$

where $T$ is the total observation time, $t_{pi}$ the duration of the $i$th peak, $n_{pi}$ the peak number, $t_{gi}$ and $n_{gi}$ being the corresponding parameters for the gaps.

Figure 1 illustrates the type of analysis that is implied (for practical reasons a slightly different procedure had to be employed) and also indicates that the operations expressed by equation 5 are only meaningful in relation to a given threshold level of concentration. The analysis was extended by firstly examining the frequency distributions of the $t_{pi}$'s and $t_{gj}$'s themselves and secondly by performing the operation at a sequence of threshold levels by automatic means (see Section 4).

It would be anticipated that both the maximum concentration and its gradient would steadily diminish with distance from the source. However, this trend is not really evident in the data, such as it is, and as mentioned earlier Barynin and Wilson observed substantial variations of sulphur dioxide concentration occurring in time intervals of ~ 1 s at 5 km downwind of a power station stack. Chatwin and Sullivan [12] have attempted to explain these and related observations by considering the physical mechanism by which turbulence causes dispersion. In their view the turbulent flow fields act in a complex way, but always so as to enhance the effect of molecular dispersion, but note however that it is only the *latter* which has the ability to *change* concentration (defined on the continuum scale). The fundamental

feature of turbulence is that the kinetic energy of the fluid motion is transferred progressively from larger to smaller scales by various mechanisms, but particularly by vortex stretching (Lumley and Tennekes [13]) — the three dimensional nature of which tends to reduce the anisotropy of the turbulent velocity components at the smaller scales. Eventually as the velocity scales become very small, about 1 mm in the atmosphere, the velocity gradients are sufficient to cause a significant destruction of energy by viscous effects and thus the turbulent energy is ultimately dissipated as heat. Hence any passive (i.e. not affecting the velocity field) material released into a fluid medium becomes involved in this complicated system of motion and the net result is generally that the material is drawn out into contorted sheets and strands — often being stretched in one direction and compressed in another. After a time the cloud of material will thus resemble a loosely wound ball of wool and, whilst its *overall* size will steadily increase, the rate of diffusion within the individual strands and sheets is slow because it depends solely on molecular diffusion. Hence the net effect of the turbulence is not actually to reduce the concentration gradients but rather to expand and regenerate the 'internal' surface area of the cloud and, by effectively *increasing* the gradients of concentration, to augment the molecular diffusion process. In many cases this latter effect is so slow that it does not preclude the existence of very high instantaneous concentrations (and gradients) at considerable distances from a source and in practice it is possible that virtually undiluted material may be observed up to several hundred metres away.

These authors also point out that spatial structure will occur down to very small scales and, even in atmospheric processes, this means fluctuations occurring over distances of as little as 1 mm. No measurements approaching this resolution have yet, to the author's knowledge, been reported in the atmosphere, but Birch et al. [14] have undertaken some interesting laboratory studies in which considerable structure was observed at these and even smaller scales. However, their results were obtained using a small methane jet (as opposed to a passively dispersing plume) and, although certain numerical results they obtained correspond quite well with those obtained by the author [2] in the atmosphere, it would be unwise to assume too close a parallel between the two situations. In the jet experiments meandering did not of course occur (since there was no very low frequency turbulence) and thus any contribution to the observed intermittency from this cause would have been excluded.

A rather different approach to the analysis and production of concentration fluctuations has been proposed by Csanady [1] and is based on the existence of an analogy between the behaviour of the variance of the concentration fluctuations and that of turbulent kinetic energy. Whilst it is plausible to expect that some relationship between these parameters will prevail it is rather difficult to justify any formal mathematical connection. This is because velocity is a vector quantity and directly related to momentum transfer (due to cross-correlation between its components) whilst the concentration

is a scalar and entirely decoupled from momentum or energy transfer processes. Csanady develops the concept mathematically and obtains an equation connecting the rate of disappearance of concentration fluctuations with that of the turbulent energy decay time and a gradient-transfer coefficient. This idea is then extended by applying the concept of self-similarity so that, in principle the concentration fluctuation variance can be predicted as a function of distance downwind and from the plume axis. In practice however, the complications of inhomogeneity in the turbulence field and of meandering, causing intermittency, make it difficult to see how this approach, notwithstanding its appeal, can be satisfactorily applied in anything but a restricted range of situations.

Turning to the future, it would seem that the statistical approach is most likely to offer the most scope as a rational basis for fluctuation description. Generally, one will be faced with non-stationary conditions and thus adjustment and probably considerable adaptation of the conventional methods of statistics will be essential if the maximum flexibility and realism in modelling is to be achieved. Horowitz and Barakat [15] discuss this aspect in relation to the estimation of the extreme values of concentration that can be expected and two procedures, based on the supposition that some fluctuation data already exists, are suggested for analysis. Despite this limitation, both procedures point the way in which it is felt the subject will develop in the next few years and thus merit attention.

The first, and somewhat difficult, method described is to actively search for and identify the non-stationary stochastic processes operating that can explain the data. As an indication of the type of philosophy required one might for example introduce diurnal, weekly or even seasonal trends into test models and check whether these improved the accuracy of matching and thence prediction. However, it is evident that a large data base may need to be accumulated in order to decipher all the non-stationary effects present — for only in this way could reliable estimates of extreme values be made.

An alternative, and in the majority of situations, more feasible approach is to select a section of the data which fulfills reasonable stationarity criteria and employ 'traditional' methods of analysis. Once some familiarity with the vagaries of fluctuation behaviour has been obtained one could then reasonably attempt to 'add on' the fluctuation statistics to the particular circumstances for which predictions were required. It is suggested that this latter method, if coupled with the physical concepts of the turbulent dispersion process proposed by Chatwin, may offer the best chance for making significant progress. The necessity to acquire enormous amounts of data in presumably a wide variety of dispersion environments to fulfil the first suggestion is clearly rather impractical. It is therefore with the latter type of approach in mind that the results presented later in this paper are discussed.

## 3. Outline of experimental method

The experimental techniques developed to release tracer material (in this case negatively ionized air) in a controlled manner and monitor its concentration downwind with the requisite time resolution have been described in detail earlier [8, 16—18] and therefore are only outlined here for the sake of completeness.

At first sight the choice of ionized air as a tracer for atmospheric dispersion investigations may seem inappropriate, nevertheless, provided its limitations are appreciated it can form the basis of a very effective, convenient and cheap system for obtaining information about plume and puff structure. Ionized air can be readily produced by exploiting the properties of corona discharges as discussed by Loeb [18], and, in the experiments reported here, was generated by creating a corona in the vicinity of fine wire ($10^{-5}$ m diameter) mounted coaxially within an earthed aluminium cylinder (diameter 0.012 m, length 0.19 m). A copious and constant supply of ions was provided by maintaining, in conjunction with the —3 kV bias to the fine wire, a current of air along the axis of the device of $\sim$ 3 m $s^{-1}$. The ion current output was —16 nA.

The ionized air concentration was determined by drawing air, at a carefully controlled rate, through a suitably biassed coaxial capacitor arrangement and monitoring the current with a sensitive amplifier. The ion collector inlet diameter was 0.036 m and the volume flow rate of air $6.67 \times 10^{-3}$ $m^3$ $s^{-1}$. With careful choice of amplifier design and biassing arrangements it proved possible to obtain good sensitivity ($\sim 10^{-10}$ C $m^{-3}$) and a response time considerably better than $10^{-2}$ s. In these experiments 1 volt was equivalent to charge concentrations of 151.35, 40.545, 15.555 and 4.995 n C $m^{-3}$ at 2, 5, 10 and 15 m downwind from the source, respectively. The concentration fluctuations were recorded on an FM instrumentation tape recorder for subsequent laboratory analysis.

## 4. Note on data analysis systems

Two essentially pragmatic methods have evolved for this purpose and although both are automated neither involves excessively complex hardware. The first system senses when the ion concentration (i.e. its equivalent voltage level) exceeds a preset threshold value upon which a counter/timer (incremental time $10^{-3}$ s) is actuated and continues until the signal voltage falls below threshold. Counting is cumulative and thus the total time the signal exceeds a given value for an entire field experiment can be determined (see Fig. 1). This sytem will be subsequently referred to as CAAS — Concentration Amplitude Analysis System. Repetition of the playback procedure for a progressively increasing sequence of threshold levels enables the concentration amplitude statistics to be built up and, in particular, frequency distributions to be calculated.

A second method of analysis, developed later, is based on a different, and complementary concept which involves the temporal (as opposed to amplitude) structure of the fluctuations (see Section 2). Again preset threshold sensing devices (ten in total) are employed but are arranged to examine the mark:space ratio(s) of the signal and here two distinct modes of operation are possible. In the first the 'mark' is examined and the duration of the concentration bursts are measured and then automatically accumulated in time 'bins'. These bins, 32 in all, are arranged in the geometrical progression (with $\sqrt{2}$ multiplier): 0.015 s, 0.015 s—0.022 s, 0.022 s—0.030 s . . . . . 5.79 min—8.19 min, > 8.19 min and thus cover most, if not all, of the time scales important in fluctuation studies. This entire sampling process can now be accomplished automatically, having been done manually originally, using an instrument developed specifically for the purpose — SHADA (Signal Height and Duration Analyser). Readout of the number of events in each time bin is a simple procedure and merely involves monitoring the memories with a digital voltmeter (1 bit $\equiv \sim$ 3 mV and so is easily resolvable). Alternatively the number distribution from all 32 bins can be automatically 'emptied' onto a chart recorder or oscilloscope if this is more convenient. The second type of analysis offered by SHADA involves a similar examination of the gap duration statistics — subsequently referred to as the burst return period distribution.

## 5. Experimental results and discussion

### *5.1 Experimental aspects*

The dispersion experiments discussed were carried out over unobstructed moorland terrain in Northern England. Meteorological conditions were heavily clouded and this, in conjunction with a mean wind speed of 5 m $s^{-1}$, indicated close to neutral stability. (Note that the choice of site was dictated entirely by topographical considerations as the equipment is completely portable and independent of mains power.) Negatively ionized air was released from the source (described in Section 3) placed at a height of 1 m above the earth's surface; equivalent to approximately 0.75 m above the top of the heather. Ion concentrations (at 1 m height) were sampled and recorded at distances of 2, 5, 10 and 15 m downwind in a sequence of four experiments each of 48 min duration.

Strenuous attempts were made to position the ion collector as close to the mean wind line downwind of the ion source as possible although fulfilment of this ambition is usually a matter of luck rather than judgement! Nevertheless the meteorological and stability conditions were sufficiently stationary to require only very minor angular adjustments (i.e. a few degrees) of the source-collector line during the sequence of experiments. Hence the results obtained should be helpful in establishing some 'baseline' parameters for simple terrain situations.

It is perhaps worth mentioning that although only four relatively short ex-

periments were carried out, implying that the numerical results presented must be at least somewhat tentative, this is to a considerable extent countered by the very high temporal resolution employed. Thus, for each 48 min period, about $2.7 \times 10^5$ data points were collected — a figure which certainly compares favourably with the majority of other diffusion investigations!

*5.2 Data processing and main results*

*5.2.1 Results obtained using CAAS and SHADA.* The intermittency, here defined as the fraction of the observation time in which the concentration was zero, was determined by playing-back the data tapes through CAAS with its threshold adjusted to a nominal zero. It was of course impossible in practice to employ a true zero voltage for this purpose because the inevitable presence of a small amount of noise and drift on the ion concentration signals would have produced spurious counts and thus led to misleading and inconsistent results. It was found, by trial and error, that for reproducible and accurate (as compared with a manual analysis of chart records) values of intermittency a threshold level of +25 mV was required. Since typical peak values of the signal were in the region of 1 V this seemed acceptable.

The amplitude-frequency distribution was determined by using CAAS with progressively increasing threshold levels (25 mV increments) up to the

TABLE 1

Mean concentration, taken over 48 minutes, as a function of distance from source (unfiltered data)

| Distance downwind (m) | 2 | 5 | 10 | 15 |
|---|---|---|---|---|
| Mean concentration ($\overline{\Gamma}$) (nC m$^{-3}$) | 4.21 | 0.525 | 0.239 | 0.159 |

TABLE 2A

Processed data from the 2 m downwind experiment[a]

| Parameter | Unfiltered | With low pass filtering | | | | |
|---|---|---|---|---|---|---|
| | | 30 Hz | 10 Hz | 3 Hz | 1 Hz | 0.3 Hz |
| $\sigma_\Gamma$ (nC m$^{-3}$) | 12.6 | 11.0 | 8.71 | 5.60 | 3.77 | 2.40 |
| $S_\Gamma$ | 4.95 | 4.87 | 4.62 | 4.31 | 4.18 | 3.93 |
| $K_\Gamma$ | 30.2 | 29.6 | 27.6 | 25.5 | 23.2 | 21.5 |
| $\hat{\Gamma}/\overline{\Gamma}$ | 36.4 | 31.9 | 25.6 | 18.4 | 13.9 | 6.74 |
| $I$ (%) | 85.2 | 82.7 | 80.9 | 78.8 | 79.1 | 86.5 |

[a] $\sigma_\Gamma$ standard deviation of ion concentration.
$S_\Gamma$ skewness of ion concentration.
$K_\Gamma$ kurtosis of ion concentration.
$\hat{\Gamma}/\overline{\Gamma}$ peak:mean.
$I$ (%) percentage intermittency.

TABLE 2B

Processed data from the 5 m downwind experiment

| Parameter | Unfiltered | With low pass filtering | | | | |
|---|---|---|---|---|---|---|
| | | 30 Hz | 10 Hz | 3 Hz | 1 Hz | 0.3 Hz |
| $\sigma_\Gamma$ (nC m$^{-3}$) | 2.21 | 2.08 | 1.83 | 1.39 | 1.03 | 0.722 |
| $S_\Gamma$ | 7.18 | 6.46 | 6.27 | 5.47 | 4.24 | 3.29 |
| $K_\Gamma$ | 66.6 | 53.3 | 51.4 | 39.3 | 23.7 | 13.0 |
| $\hat{\Gamma}/\Gamma$ | 78.2 | 62.7 | 58.9 | 43.4 | 22.2 | 10.6 |
| $I$ (%) | 90.1 | 87.9 | 82.6 | 84.8 | 81.0 | 82.9 |

TABLE 2C

Processed data from the 10 m downwind experiment

| Parameter | Unfiltered | With low pass filtering | | | | |
|---|---|---|---|---|---|---|
| | | 30 Hz | 10 Hz | 3 Hz | 1 Hz | 0.3 Hz |
| $\sigma_\Gamma$ (nC m$^{-3}$) | 0.818 | 0.765 | 0.679 | 0.536 | 0.395 | 0.279 |
| $S_\Gamma$ | 8.82 | 7.82 | 7.48 | 5.62 | 4.49 | 3.50 |
| $K_\Gamma$ | 129 | 97.0 | 89.8 | 47.0 | 30.6 | 14.9 |
| $\hat{\Gamma}/\Gamma$ | 112 | 90.4 | 79.0 | 48.0 | 28.5 | 12.2 |
| $I$ (%) | 83.7 | 83.9 | 85.2 | 83.7 | 83.7 | 85.2 |

TABLE 2D

Processed data from the 15 m downwind experiment

| Parameter | Unfiltered | With low pass filtering | | | | |
|---|---|---|---|---|---|---|
| | | 30 Hz | 10 Hz | 3 Hz | 1 Hz | 0.3 Hz |
| $\sigma_\Gamma$ (nC m$^{-3}$) | 0.346 | 0.329 | 0.310 | 0.254 | 0.211 | 0.179 |
| $S_\Gamma$ | 5.38 | 5.06 | 4.79 | 4.26 | 3.91 | 4.12 |
| $K_\Gamma$ | 42.1 | 38.0 | 32.1 | 23.3 | 19.6 | 23.0 |
| $\hat{\Gamma}/\Gamma$ | 43.5 | 42.7 | 34.1 | 19.2 | 13.7 | 10.6 |
| $I$ (%) | 71.0 | 72.8 | 73.5 | 72.1 | 68.6 | 71.2 |

highest peak level on the particular recording involved and the parameters presented in Tables 1 and 2 were calculated. Also included in the latter table are the results of a later analysis in which the procedure was repeated with a high quality (48 dB attenuation per octave) low pass filter interposed between the tape recorder output and the CAAS input. The main objective of this was to evaluate, quantitatively, the effect of detector response time on the nature of the concentration fluctuations perceived, see also Figs. 2, 3, 4 and 5.

In theory the mean value of concentration should be independent of filtering, but in practice, mainly due to the finite threshold increment, this

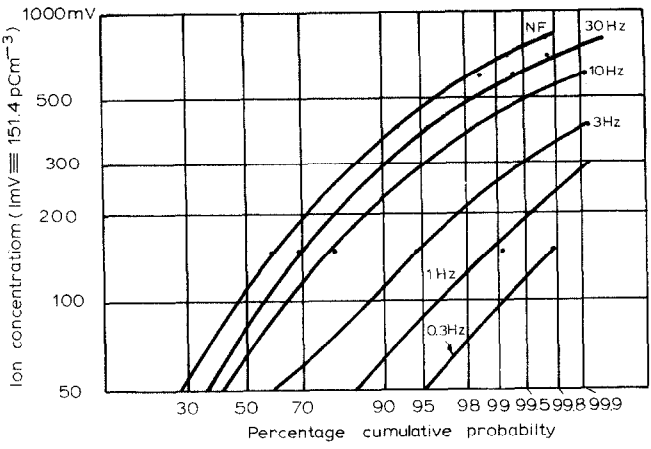


Fig. 2. Ion concentration frequency distributions at 2 m downwind.

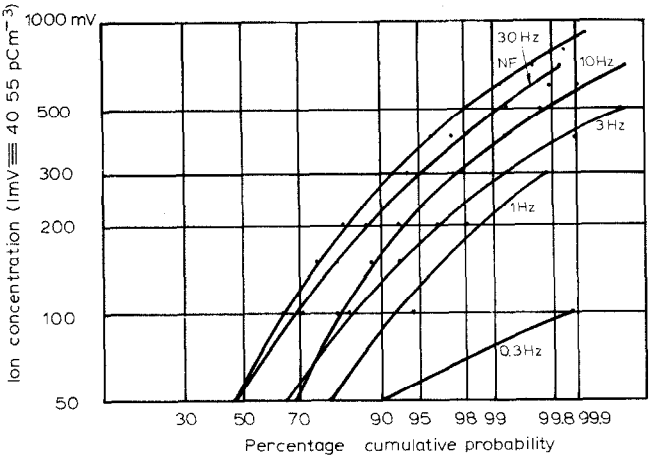


Fig. 3. Ion concentration frequency distributions at 5 m downwind.

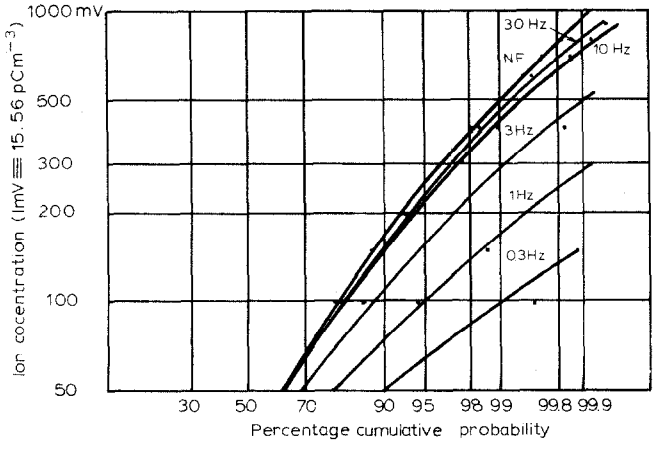


Fig. 4. Ion concentration frequency distributions at 10 m downwind.

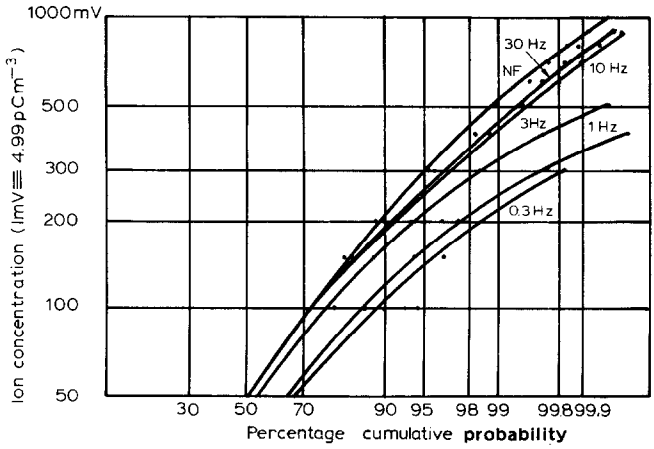


Fig. 5. Ion concentration frequency distributions at 15 m downwind.

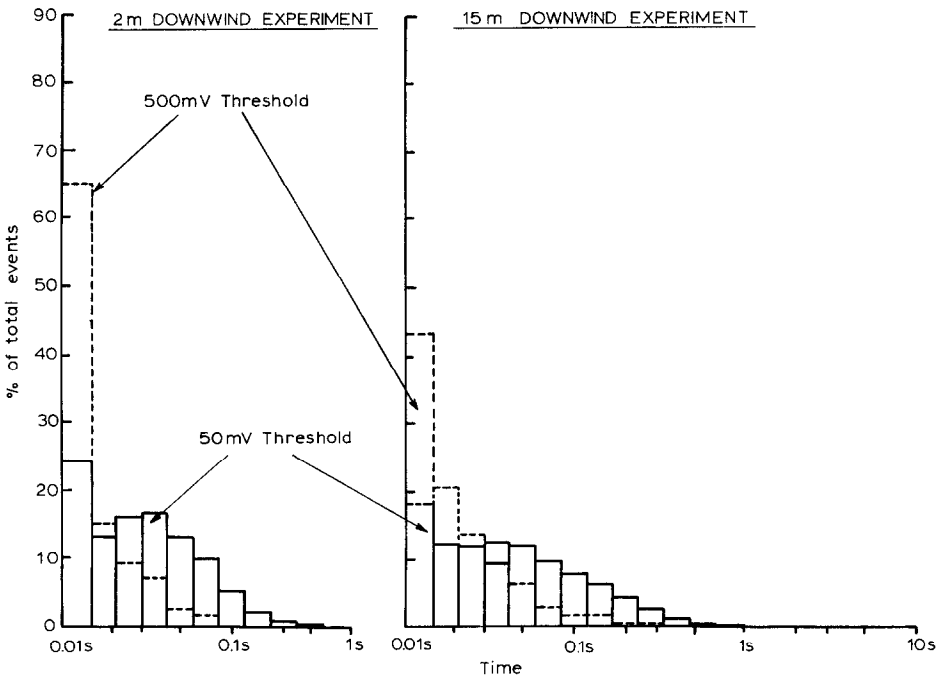


Fig. 6. Burst length distributions obtained using 'SHADA'.

was not quite so. However the discrepancy between means obtained with various filtering bandwidths was never greater than about 10% and this was regarded as acceptable.

A representative selection of results obtained with SHADA is presented in Figs. 6, 7 and 8. Table 3 below shows, in addition, the behaviour of the event total (i.e. the sum of the event counts in each of the time bins) for the

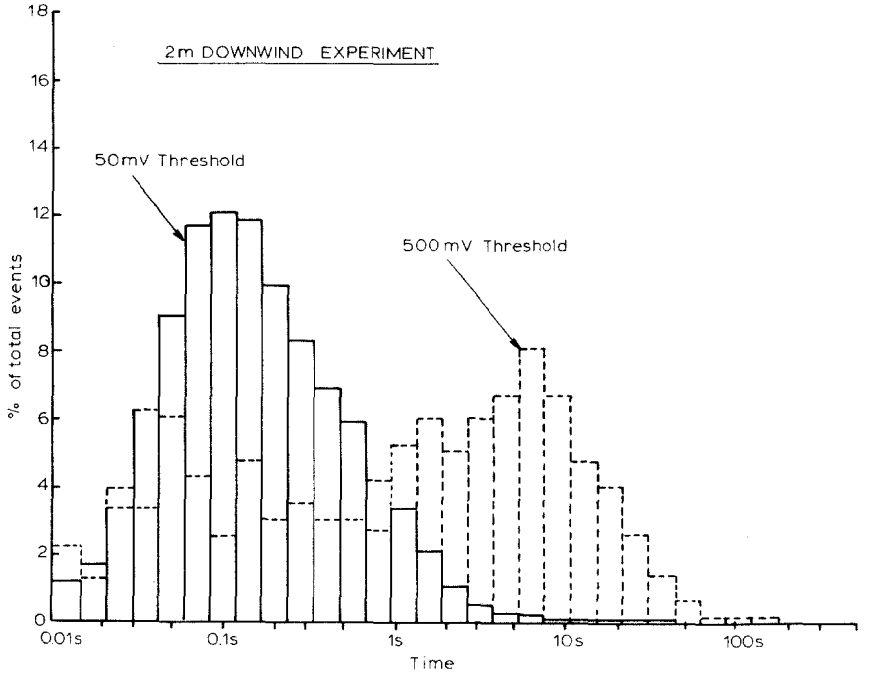


Fig. 7. Burst return period distributions obtained using 'SHADA'.

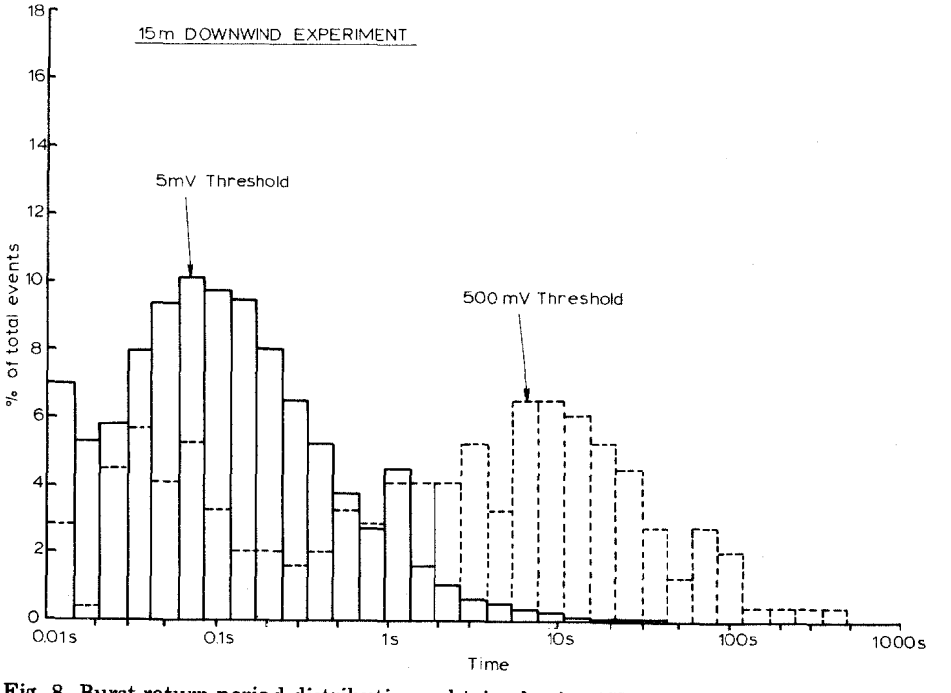


Fig. 8. Burst return period distributions obtained using 'SHADA'.

TABLE 3

Total event count as a function of threshold voltage

| Threshold level | Total even count | | | |
|---|---|---|---|---|
| (mV) | 2 m | 5 m | 10 m | 15 m |
| 50 | 9132 | 2892 | 4242 | 7750 |
| 100 | 7464 | 2221 | 2219 | 4583 |
| 200 | 5075 | 1352 | 1078 | 2322 |
| 300 | 2873 | 723 | 500 | 830 |
| 400 | 1633 | 435 | 310 | 494 |
| 500 | 625 | 211 | 155 | 245 |
| 800 | 49 | 23 | 38 | 46 |
| 1000 | 3 | 5 | 13 | 7 |
| 1500 | 0 | 0 | 2 | 0 |

experiments over all the threshold levels used. The values given in the Table were derived from the burst length data.

*5.3 Discussion*

*5.3.1 Mean concentration.* The discontinuous nature of the concentration fluctuations suggests that it could be instructive to define two distinct types of mean. The conventional approach, i.e. to average the observed values over the entire experimental period, leads to the results in Table 1. However, this produces averages which are sensitively dependent on the angular relationship between the detector and the mean wind vector and there is thus a rather unsatisfactory degree of arbitrariness about them. In other words if the detector had been sited, fortuitously, very close to the mean wind line then a higher value of 48 min mean concentration would be obtained than if it had been placed off-axis.

A way of defining the mean concentration*, which at least circumvents this difficulty, is to perform the averaging process only over the intervals when the concentration is non-zero. This approach, which is closely equivalent to finding the average concentration within the plume, yields the results in Table 4, which were obtained using the relation

$$\bar{\Gamma}(\text{plume}) = \frac{\bar{\Gamma}}{1 - \frac{I}{100}} \tag{5}$$

Comparison of Tables 1 and 4 indicates that the decline of mean concentration with distance is rather more regular for the 'in plume' averages:

*Another possibility, which could be examined in future experiments, might be to use several ion collectors, and then interpolate the results to find the position of maximum mean concentration.

presumably this is a result of removing the unpredictable effects of meandering.

TABLE 4

Mean concentration in the plume for the four experiments

| Distance downwind (m) | 2 | 5 | 10 | 15 |
|---|---|---|---|---|
| $\overline{\Gamma}$(plume) (nC m$^{-3}$) | 28.4 | 5.33 | 1.46 | 0.549 |

*5.3.2 'Instantaneous' plume radii.* Visual examination of concentration-time records shows several common yet distinct features and this tempts one to try to deduce the actual plume dimensions for the following reasons. Generally, on entering the plume, a very rapid rise in concentration occurs — typically the concentration changing from near zero to a high value within a few tens of milliseconds. Thereafter, although very substantial variations in concentration are usually observed — due to either repeated transections of the plume or the presence of internal structure or more likely both; in a number of cases the concentration appears to remain reasonably uniform well inside the plume. Hence, provided the ion source strength ($i$) and the mean wind speed ($\bar{u}$), are known, it is theoretically possible to estimate a *mean* 'instantaneous' plume radius, $R_{\text{inst}}$, using the charge conservation principle. Hence

$$R_{\text{inst}} = \left[ \frac{i}{\pi \, u \, \overline{\Gamma}(\text{plume})} \right]^{1/2} \tag{6}$$

where it has been assumed, and this is substantially confirmed by smoke tracer experiments, that the plume cross-section is approximately circular. Table 5 shows the values of this quantity obtained with $|\,i\,| = 16$ nA and $\bar{u} = 5$ m s$^{-1}$ which were appropriate to these experiments.

In the past [20] it has often been the practice, in order to facilitate modelling and prediction, to fit power laws to the relationship between plume

TABLE 5

Calculated values of 'instantaneous' plume radii

| Distance downwind (m) | 2 | 5 | 10 | 15 |
|---|---|---|---|---|
| Instantaneous plume radii, $R_{\text{inst}}$ (m) | 0.190 | 0.437 | 0.834 | 1.36 |
| $R_{\text{inst}}$, corrected for electrostatic expansion: $R_{\text{inst}}$ (m) | 0.118 | 0.351 | 0.762 | 1.18 |

width and distance downwind from source. Adopting this procedure here yields a best fit power law, obtained using a least squares regression technique, of

$$R_{inst} = R_0 + 0.087x^{0.996} \tag{7}$$

where $R_0$ is the plume radius at the release point, i.e at $x = 0$, and thus corresponds to the ion generator outlet radius (0.013 m).

An obvious limitation to the application of eqn. 7 is that it refers to an electrically charged plume and, whilst in fact many industrial stack plumes are very highly charged [20], the result would be more useful if the electrostatic effects could be quantified and then removed. Provided certain assumptions can be justified, and these are not unduly restricted, it is possible to deduce that,

$$R_{turb} = R_0 + Ax^p - \frac{ui}{2\bar{u}^2 \pi \epsilon_0} \int_0^x \frac{dx}{R_0 + Ax^p} \tag{8}$$

as shown in the Appendix. In the equation the constants $A$ and $p$ are those in the power law expansion expression, $x$ is the distance downwind and $R_{turb}$ the corrected radius.

Equation 8 was integrated numerically and the results obtained are also listed in Table 5. As before it is possible to determine best fit values to a modified power law description for the corrected radius and one finds that

$$R_{turb} = R_0 + 0.046x^{1.21} \tag{9}$$

It is noteworthy that the value of the index in this equation considerably exceeds those commonly accepted for the power law expressions for plume expansion — which are generally in the region of 0.8—0.9. However, these are invariably derived from 'mean' plume data and thus cannot really be compared with the present results. Nevertheless it is not likely that the trend expressed in equation 9 can be maintained out to distances much in excess of 100 m or so since, even at that distance, the predicted plume radius ($\sim$ 12 m) is somewhat too large. A possible explanation for this discrepancy may be in the relation between the observed range of plume size (i.e. $\sim$ 0.1—1.0 m) and the dominant turbulent energy scales. This ratio would appear to exert a substantial influence on the rate of plume growth and further must in itself be a function of the plume size. In fact Csanady [1] also mentions a rapid growth phase in his discussion of puff dispersion which appears to originate from the same phenomenon.

*5.3.3 Statistical moments, intermittency and peak to mean ratios.* Tables 2A, B, C and D give values for these parameters as a function of distance from source and also illustrate the effect of low pass filtering. Some not unexpected trends can be discerned, in particular the progressive reduction in $\sigma_\Gamma$ with distance. Note, however, that the corresponding coefficients of variation (or

relative intensity) of the fluctuations vary from 3.03, 4.22, 3.42 and 2.17 at 2, 5, 10 and 15 m respectively and thus fall off much more slowly with distance. (The correlation coefficient between them is in fact —0.59.) Further if the mean concentration *in the plume* is used as the basis for calculating the relative fluctuation intensity then these values become respectively 0.45, 0.42, 0.56 and 0.63. Here the correlation coefficient is +0.94 thus suggesting a slight but systematic increase with distance downwind from the source. (A least squares regression analysis yields the relation $I(x) = 0.02x + 0.39$.)

The ratios between the $\sigma_I$'s for the unfiltered and 0.3 Hz values are 5.25, 3.06, 2.93 and 1.93 at the four distances downwind the correlation coefficient being, in this case, —0.89. Hence these results appear to be consistent with a systematic shift towards longer scales as dispersion proceeds. However, the more sophisticated and physically realistic descriptions of this process discussed in Section 2 indicate that this may be an oversimplification and the true explanation for the observed trend may be more subtle.

In all the experimental results the fluctuation statistics are markedly positively skewed, typical values being in the region of 7 for the unfiltered data. Note that these values have been normalized by their respective standard deviation raised to third power and thus direct comparisons between experiments are permissible. No very obvious trends with distance are evident, the correlation coefficient being only +0.13, however, a fairly systematic reduction in skewness with increased filtering is apparent.

Similar comments also apply to the kurtosis — the very high values reflecting the 'peaky' nature of the distribution. Again no significant trend with distance emerges, the correlation coefficient being +0.23.

Values of peak to mean concentration ratio were obtained by noting the maximum threshold level (during CAAS processing) at which a non-zero count was maintained. Although the internal clock in this system operates in $10^{-3}$ s increments, information was only recorded in 0.1 s intervals in order to minimise the risk of any isolated very short duration spurious transients (due to for example a charged dust particle entering the ion collector) producing misleading results. Nevertheless it is theoretically possible for a single peak of only 0.1 s length actually to determine the peak to mean ratio obtained during an entire 48 min experiment. Consequently the numerical values of this ratio tend to be variable and the reader is cautioned not to attach too much significance to individual results. In practice, it usually happens that the peak level occurs two or three times during an experiment — the implication being that 'experiencing' the peak is an unlikely event — typically the probability of doing so being ~ 1 in $10^5$. However, even though it is an apparently rare event the fact that such high instantaneous concentrations can occur is obviously important for the accurate assessment of flammable and toxic risks and odour nuisance particularly. (No significant trend of peak:mean with distance is evident; the cross correlation coefficient being +0.13.)

One aspect of considerable theoretical interest concerns the relationship

between the peak concentrations observed downwind and that at release. If concentrations approaching that at source are observed it would lend support to the mechanism of turbulent dispersion put forward by Chatwin and described earlier in Section 2. However, for an electrically charged tracer some form of correction must be applied to compensate for the effects of electrostatic repulsion before comparisons can be made. A convenient method of analysis is to assume that the ion plume spreads by repulsion alone, i.e. there are no additional dispersive processes operative, calculate the ensuing ion concentration using the formula [16],

$$\Gamma(t) = \Gamma_0 \Big/ \left( 1 + \frac{\mu \Gamma_0 t}{\epsilon_0} \right) \tag{10}$$

and then compare the results obtained with the peak values actually observed, see Table 6. (In eqn. 10, $\Gamma_0$ is the concentration at release and $\Gamma(t)$ that at a time $t$ after release.) Note that in Table 6 the theoretical maxima were calculated with an assumed mean wind speed of 5 m $s^{-1}$. Hence the estimates could probably be in error by as much as 30% since it is the instantaneous speed which determines the transit time between ion generator and collector.

TABLE 6

Comparison of theoretical maximum ion concentration with those actually observed

| Distance downwind (m) | 2 | 5 | 10 | 15 |
|---|---|---|---|---|
| Theoretical maximum concentration (nC $m^{-3}$) | 110 | 44.1 | 22.1 | 14.7 |
| Peak value observed (nC $m^{-3}$) | 153 | 41.0 | 26.7 | 6.92 |

Nevertheless these results suggest quite definitely that it is possible to observe, occasionally, completely undiluted material at least within 10 m of the source and probably much further. If this is in fact the case, and a more recent series of experiments appears to substantiate this, then again there are implications for many areas of hazard and nuisance assessment.

*5.3.4 Cumulative concentration probability distributions.* Figures 2, 3, 4 and 5 show the distributions obtained at the four distances for each of the six bandwidths used. These distributions are plotted in terms of mV rather than in ion concentration units — see the conversion factors in Section 3. Note, that in developing these distributions, non-zero values of concentration have been discounted, because of the inherent difficulty of handling zero quantities on a logarithmic scale. Some curvature is apparent on the figures suggesting that adherence to the log—normal distribution is by no means perfect. It is possible that this deviation may, at least partly, be due to the nature of the tracer used but this is certainly not the sole reason because, if

it were, the discrepancy would tend to be smaller at the longer distances, where ionic repulsion effects have by then become virtually negligible. In any case, the theoretical justification for expecting a log—normal distribution is rather questionable and it is mainly a matter of convention that the results are presented in this format. (It is arguable that the use of a linear axis may have been an equally acceptable choice — possibly superior in that it would allow the reader to come to his own conclusions about the nature of the distribution without having the fashionable log—normal foisted upon him!)

Aside from this rather contentious aspect the effect of filtering is quite unambiguously illustrated by the progressive diminution in the probability of observing high peak values together with a reduction in slope —reflecting a decrease of (geometric) standard deviation. In particular note the tendency towards bunching of the curves as the distance increases — presumably being a result of the loss of high frequency structure as one moves away from the source.

*5.3.5. Temporal structure analysis using SHADA.* Table 3 details the total events (i.e. the sum of all the counts in the individual time bins) for the four experiments and sequence of threshold values used. (Note that these totals do not, at least in theory, depend on whether 'burst length' or 'burst return period' is considered because the summation should yield the same or very nearly the same result. Experimental results did in fact support this assertion.) It would seem there ought to be at least a tenuous connection between the total events and intermittency (note, however, that the latter has been defined on the basis of a 25 mV threshold) because, to take an extreme case as an example, if the bursts were all of identical length, then the event total and intermittency would behave in complementary fashion. Comparison of Tables 2 and 3 indicates that such a trend is not really discernible (correlation coefficient —0.52), thus suggesting that the intermittency can remain high even though much fluctuation activity (i.e. many events) has occurred and vice versa.

The 2 m downwind experiment burst length distribution taken at 50 mV threshold contains a rather ill-defined most probable value in the 0.30—0.42 s interval; the higher level occurring in the lowest class ($< 0.015$ s) being due to the presence of high frequency noise. However at 500 mV the most probable value shifts to the shortest class interval and this effect is certainly a reflection of the pulse shape itself and not related to spurii. Note also that the total events at the higher threshold is much smaller, by a factor of nearly 15, thus implying that only about 7% of the bursts exceeded 500 mV in amplitude. Further, the longest burst observed throughout the 48 min run at the 500 mV load is a full 4 class intervals (i.e. $(\sqrt{2})^4$, $4\times$) shorter than at 50 mV.

These results also provide some important clues regarding the burst or pulse shapes occurring in the fluctuations. If, for example, the pulses were rectangular and of similar, amplitude, then no change in the length distribu-

tion or event number would have occurred with threshold variation until the latter exceeded the pulse height. The existence of a rapid fall-off of these parameters in practice strongly suggests that the pulse shape is triangular — i.e. the structure is peaky — a feature also evinced by the large kurtosis values observed.

Similar behaviour is evident in the 15 m histograms. However here, the distributions are broader and bursts of up to $(\sqrt{2})^5$ i.e. 5.7 × the duration of the longest seen in the 2 m experiment were observed. This feature may be related to the increased plume width at the longer distance and in fact this ratio, 7.2, accords quite well with the burst length increase.

Burst return period data are given in Figs. 7 and 8 and provide complementary information to that above. In particular, since return period analysis is essentially an examination of the statistics of the gaps in the concentration distribution it is thus a far more precise technique for describing the intermittency than merely specifying a global percentage value. Alternatively, particularly in the context of hazard assessment, one can view this type of analysis as providing an indication of how long one has to wait before a given value of concentration is likely to recur.

The nature of the distributions themselves is rather different to those of burst length. For instance in the case of the 2 m downwind experiment with 50 mV threshold, there is some tendency towards a log—normal distribution since the histogram appears to have roughly Gaussian form on its logarithmic variate scale. However this could be fortuitous since the other three distributions are markedly skewed: negatively for both 500 mV results and positively for 15 m, 50 mV data. Perhaps the most striking feature is the marked shift to longer values of return period with the increase of threshold in both the 2 and 15 m case, the most probable value being displaced by almost 2 orders of magnitude. Even then, however, at the relatively high concentration equivalent to 500 mV (in comparison with the overall mean) one has only to wait, *on average*, about 8 s for the same levels to be experienced again. This does not preclude the existence of some very long gaps as in both cases the distribution extends out to several minutes — physically this being the result of large horizontal eddies causing the plume to meander. Some tendency towards bimodality can be seen in both the 500 mV analyses — the shorter peak at about 0.1 s possibly coinciding with some feature of the internal plume structure.

## 6. Conclusions

The results presented in this paper confirm the following main features of instantaneous plume structure:

(i) Very high levels of intermittency, typically 80—90%, coupled with correspondingly large peak to mean ratios in the range 30—150.

(ii) Plumes, and therefore by implication, puffs are generally of small cross-section and in the former case have a sinuous form. Consequently the con-

centration, when within them, is high and moreover the time mean (i.e. averaged over 10—15 min) of concentration is actually accumulated in the form of a series of short, discontinuous but intense bursts of concentration. This has relevance to many applications of dispersion analysis but particularly for the accurate assessment of flammability/explosion and toxic risks and nuisance due to malodours.

(iii) Detector response time is a crucial factor in determining the impression obtained of plume structure — a rapid reduction in all the statistical parameters relating to the variability and peakiness of the fluctuation being noted when the response is deliberately degraded by the introduction of a low pass filter.

Finally the point should be made that although the experiments on which the above conclusions have been developed were performed at close ranges there are certain theoretical reasons, mostly founded on self-similarity and related postulates, for asserting that many of the structural features observed will persist for considerable distances downwind. In addition the results of more recent experiments having source-detector separations of several hundred metres indicate the existence of similar (and just as much) fine structure and thus lend further support to this assertion.

## Appendix

*Power law expression for instantaneous plume radius: examination of electrostatic repulsion effects*

The radial electrostatic field due to the net charge contained in the plume causes radial and, to a much lesser extent, longitudinal expansion. The latter can safely be ignored [16], but the radial component can be comparable with the expansion due to turbulence and thus requires investigation. If the plume, for simplicity, is considered to be a uniformly charged cylindrical volume then, in a *non-turbulent* flow, it can be shown, using the fundamental equations of electrostatics, that,

$$\left(\frac{\partial R}{\partial x}\right)_{\text{electrostatic}} = \frac{\mu i}{2 R \bar{u}^2 \pi \epsilon_0} \tag{A1}$$

where $(\partial R/\partial x)_{\text{electrostatic}}$ is the rate of increase of plume radius with distance $(x)$, $\mu$ the ionic mobility, $i$ the output current of the ion generator, $\bar{u}$ the flow velocity and $\epsilon_0$ the permittivity of free space. It must be stressed that equation A1 is only an approximation to reality, in practice the charge is not uniformly distributed and neither is the wind speed constant, but nevertheless it provides a useful indication of the relative magnitudes of the dispersive agencies operating on the plume.

If the flow is turbulent, as is generally the case in the atmosphere, then the total, and therefore *observed*, plume expansion rate can be written

$$\frac{dR}{dx} \simeq \left(\frac{\partial R}{\partial x}\right)_{\text{electrostatic}} + \left(\frac{\partial R}{\partial x}\right)_{\text{turbulent}} \tag{A2}$$

where $(\partial R/\partial x)_{\text{turbulent}}$ represents the contribution to plume expansion arising directly from turbulent processes. Thus

$$\left(\frac{\partial R}{\partial x}\right)_{\text{turbulent}} \simeq \frac{dR}{dx} - \frac{\mu i}{2 R \bar{u}^2 \pi \epsilon_0} \tag{A3}$$

and integrating

$$R_{\text{turbulent}} \simeq R - \frac{\mu i}{2 \bar{u}^2 \pi \epsilon_0} \int \frac{dx}{R} \tag{A4}$$

Since $R$ refers to the observed radius it can be replaced by the power law approximation already deduced (i.e. eqn. 7) and eqn. A4, with this modification, can then be integrated numerically to reproduce the results given in Table 4.

## References


1 Csanady, G.T., Turbulent diffusion in the environment, D. Reidel, Dordrecht, Holland, 1973.
2 A.A. Townsend, The Structure of Turbulent Shear Flow, 2nd edn. Cambridge University Press, Cambridge, 1976.
3 C.D. Jones, Statistics of the concentration fluctuations in short range atmospheric dispersion, Conference on "Mathematical modelling of turbulent diffusion in the environment". Liverpool University Sept 12—13, 1978. Proceedings published by Academic Press, C.J. Harris, Ed.), 1978.
4 J. Murlis and C.D. Jones, Fine-scale structure of odour plumes in relation to insect orientation to distant pheromone and other attractant sources, Physio. Entomol., 6 (1981) 71.
5 P.C. Chatwin, The use of statistics in describing and predicting the effects of dispersing gas clouds, J. Haz. Mat., (1982) to be published.
6 J.A.M. Barynin and M.J.G. Wilson, Outdoor experiments on smell, Atmos. Environ., 6 (1972) 197.
7 A. Hadjitofi and M.J.G. Wilson, Fast response measurements of air pollution, Atmos. Environ., 13 (1979) 755.
8 C.D. Jones, Ion concentration variations at short distances downwind of continuous and quasi-instantaneous point sources, Pestic. Sci., 8 (1977) 84.
9 F.A. Gifford, Statistical properties of a fluctuating plume dispersion model, in F.N. Frenkiel and P.A. Sheppard, eds., Atmospheric Diffusion and Air Pollution, Advances in Geophysics, 6, Academic Press, New York, 1959, p. 117.
10 J.L. Lumley and H.A. Panofsky, The structure of atmospheric turbulence, John Wiley and Sons, London, 1964.
11 G.J. Cats and A.A.M. Holtslag, Prediction of air pollution frequency distributions, Atmos. Environ., 14 (1980) 255.
12 P.C. Chatwin and P.J. Sullivan, On the probability density function of concentration in turbulent dispersion, Transactions of the CSME, 5 (78—79) (1979) 192.

13 J.L. Lumley and H. Tennekes, A first course in turbulence, MIT Press, London, 1972.
14 A.D. Birch, D.R. Brown, M.G. Dodson and J.R. Thomas, The turbulent concentration field of a methane jet, J. Fluid Mechanics, 88 (1978) 431.
15 J. Horowitz and S. Barakat, Statistical analysis of the maximum concentration of an air pollutant: effects of auto-correlation and non-stationarity, Atmos. Environ., 13 (1979) 811.
16 C.D. Jones and W.C.A. Hutchinson, Plumes of electric space charge in the lower atmosphere, J. Atmos. and Terr. Phys., 38 (1976) 485.
17 C.D. Jones, Ionized air as a wind tunnel tracer, J. Phys. E: Sci. Instr., 10 (1977) 1287.
18 C.D. Jones and N.T. Gulliford, Developments in the use of ionised air as a wind tunnel tracer, J. Phys. E: Sci. Instr., 12 (1979) 321.
19 L.B. Loeb, Electrical Coronas: their basic physical mechanisms. Univ. of California Press, Berkeley and Los Angeles, USA, 1965.
20 F. Pasquill, Atmospheric Diffusion, 2nd ed., Ellis-Horwood, Chichester, UK, 1974.
21 C.D. Jones and S.G. Jennings, Large Electric fields due to industrial chimney stack plumes, Atmos. Environ., 11 (1977) 1197.